Proceedings of 2022 IEEE
International Conference on Mechatronics and Automation
August 7 - 10, Guilin, China

Simulation analysis of flexible grippers in vascular interventional surgery robot

Chuqiao Lyu, Shuxiang Guo*, Chenguang Yang, Yue Wang, Yonggan yan
Key Laboratory of Convergence Biomedical Engineering System and Healthcare Technology,
The Ministry of Industry and Information Technology, School of Life Science, Beijing Institute of Technology,
No.5, Zhongguancun South Street, Haidian District, Beijing 100081, China
E-mails: { guoshuxiang & lyuchuqiao }@bit.edu.cn;
* Corresponding author

***Abstract*—The vascular interventional surgery robot (VISR) can protect surgeons from radiation exposure. The robot provides high-precision guidewire/catheter control during the operation, but its flexibility is still not as good as that of human fingers. The main reason is that the robot cannot accurately control the guidewire/catheter and measure the clamping force at the same time. Another problem is that the rigid surgical instruments will not respond to pressure changes in time, which was easy to cause endovascular damage. In order to solve this problem, a parallel multi-fingered flexible gripper structure was proposed. The small-sized gripper can stably clamp the guidewire/catheter in a narrow surgical space. By simulating the clamping process with Mooney-Rivlin model, the suitable size of grippers for operation is selected. In addition, the simulation results show that the clamping deformation can be controlled by changing the moving distances, which will directly affects the range of the maximum sliding stress. It means that the propose flexible gripper can cushion the sudden stress in surgery and provide more flexible functions for deploying surgical robots.**

***Index Terms*—vascular interventional surgery robot, flexible gripper, simulation analysis, Mooney-Rivlin.**

I. INTRODUCTION

Vascular interventional surgery is an effective method for the treatment of cardiovascular and cerebrovascular diseases, such as thrombosis and stroke. However, surgeons who perform interventional procedures often face the risk of occupational diseases caused by radiation exposure. In recent years, the teleoperation of vascular interventional surgery robot (VISR) as a friendly way of the surgeon's health is widely used in clinical [1]–[4]. On the one hand, surgeons is far away from the operating table, and operate the rocker to command robots [5], [6]. On the other hand, the robot holds the soft and slender catheter/guidewire, and repeats surgeon's movements. Some studies [7], [8] have shown that increasing the force transmission between the master and slave can improve the surgeon's sense of surgical presence. One difficulty is that VISR needs to accurately measure the stress changes on the catheter/guidewire, and timely feedback to the hands. The famous solution is to separate the load cell from the clamping device [9]–[11]. The mechanical actuator has precise movement, but the disadvantage is that the rigid jaw structure easily leads to catheter deformations [12].

Some studies discussed that motor will vibrate during the movement due to the separation of clamping points and force measuring points. In addition, the traditional rigid gripper has no force buffer, and its response speed to sudden stress change is slow. These serious abnormal situations often occur in catheter operations, causing vascular injury and even punctures. At present, according to the different operating force ranges of catheter/guidewire, a multi-level operation strategy is proposed [13]. However, the strategy needs to be equipped with a high-performance servo motion controller, which undoubtedly increases the difficulty of system design. Sometimes, the surgeon's hand are easy to tremble and the operation is not skilled [14]–[17]. Inaccurate motion capture increases the risk of operation. It is also worth noting that the separation of clamping and force measurement will increase the volume of VISR, which will cause inconvenience.

Robot end effector with grasping function can be divided into active and passive. The active grippers can be used to move objects of general shape, such as torsion [18]. Passive grippers need more structural and dimensional design to meet specific operation requirements [19]. Some studies [20] have shown that the flexible passive gripper has stronger adaptability to objects of different shapes. By contacting surfaces and objects with low hardness, the flexible grippers can ensure the integrity of fragile objects, which is most widely used in clamping foods [21]. More importantly, by measuring the deformation of the surface, additional tactile information can be collected. Some researchers [22] measure the force of the target in different directions by using superelastic material. The magnitude and direction of the force can be observed through the changes of the mark points. In some studies, the isotropic hyperelastic objects can be restrained by gas, and maintain a constant grip strength through friction [23].

In VISR, the robot needs to clamp, rotate and transport the soft catheter/guidewire, which makes the gripper at a high level in terms of size and performance.

Therefore, this paper give some reasons for the design of flexible clamping actuator:

- The rigid surface is easy to damage catheters, and will be affected by mechanical motion.

- The traditional clamping action lacks buffer capacity and can not respond to stress changes in time.
- Separation of clamping point and measuring point increases the volume of the robot, which brings inconvenience to the operation.

In this paper, based on the two-parameter hyperelastic Mooney-Rivlin model, a simulated flexible gripper is built. It is used to estimate the clamping force of flexible clamping material surface deformation on catheter and guidewire. The radial force is transmitted by the moving distance between two symmetrical clamps. By changing the moving distance, the grippers can control the maximum friction range of catheter/guidewire and ensure safe advancements in the blood vessel. This article mainly includes the following parts: the second part introduces the structure and the simulation parameters of the owner in detail; The third section shows the relationship between the movement and stress of the gripper; In the fourth section, we will discuss the practicality of flexible gripper in VISR, and finally, draw a conclusion in the fifth section.

II. Gripper simulation

Because the catheter/guidewire in interventional surgery is soft and slender, surgeons often need to perform multi-fingering operation to maintain smooth control of the moving blood vessels. As shown in Fig. 1(b), when the surgeon grasps the guidewire, the translation is realized through the thumb and forefinger, and the retraction is realized through the other three fingers. During exercise, the hand always grasps the guidewire with fingers, and can only move in a narrow space. In order to keep the stability of catheter/guidewire and improve the movement efficiency of robot, it is necessary to increase the grasping area of the end effector. Similarly, the movement space of the end-effector needs to be limited, which means that the size and movement range of the gripper need to be optimized. Therefore, the following three constraints are assumed to establish the simulation model of flexible gripper:

- The girppers needs to increase the contact area of the retaining catheter/guidewire as much as possible.
- The flexible structure need to buffer the translation and retraction, and also ensure sufficient clamping force by optimizing the size.
- According to the operation space of the human hand, the motion space of the girppers is preset in the rectangular space of $80mm \times 60mm \times 40mm$.

A. Structural design

According to the above conditions, a flexible gripper structure with side-by-side and staggered traction fingers is proposed. Fig. 1(a) shows details of this structure, in which the black central cylinder represents the guidewire, while the white parts at the left and right sides represent the clips. Each clamping part contains a series of side-by-side thin pulling fingers, in which an odd number of pulling fingers (N, in Fig. 1, $N = 5$.) are used for one clamp. The other gripper has a even number of fingers ($N + 1$), and the width of the outer finger is half that of the inner finger. It is to ensure that the pulling force received on both sides of grippers is equal and acts in the same position. Fig. 1(c) shows the influence of deformation of flexible material. We assumes that the grippers can be driven by external components. When the grippers are tensioned, the deformation of the flexible material completely wraps the central part of the guidewire and provides enough clamping force. It can be easily seen that the clamping force is related to the size and displacement of the gripper. We will show the detailed information in the third section.

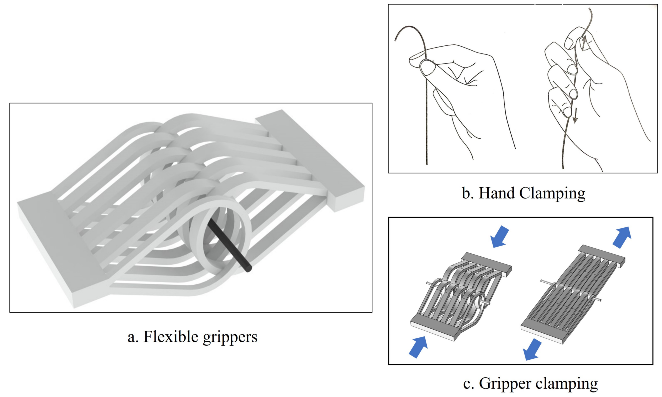

Fig. 1. The flexible grippers

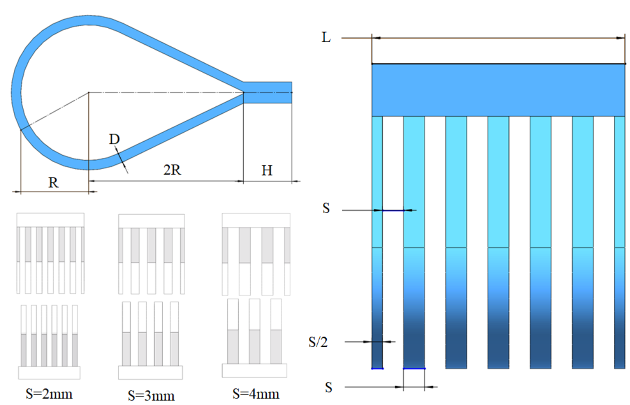

Fig. 2. The gripper sizes

The parameters of gripper size are described in Fig. 2, where R is the outer diameter of the arc at the front of a single finger. The distance from the front half to the fixed finger is set to $2R$, including a circular arc and a tangent; D stands for the thickness of the finger; H stands for the width of the fixed finger, which is a fixed value of $5mm$; At the same time, it is easy to know that the height of the fixed finger is $2D$; L stands for the width of the gripper, which is a fixed value of $24mm$; Therefore, when the width of the pulling fingers S changes, the number of pulling fingers N on the gripper will also change. In the lower left corner of Fig. 2, we have drawn the state of two grippers when $S = 2mm$, $S = 3mm$ and $S = 4mm$. During the process of clamping, they always keep the same clamping area on the guidewire.

B. Hyperelastic model

The end-effector of medical robots needs to use human friendly materials. silicone rubber is widely used in the manufacturing process of medical equipment, and it is suitable as the manufacturing material of flexible clamps. Because of the superelastic characteristics of silicone rubber, its stress-strain relationship is nonlinear. In order to study the relationship between the clamping force provided by the gripper through traction and the clamping distance, this part introduces a two-parameter Mooney-Rivlin model simulation model based on uniaxial tension. First of all, note that for an incompressible hyperelastic object, the elastic strain energy W of the gripper can be expressed by the stretching ratio λ.

$$W = f(\lambda) \tag{1}$$

In isotropic materials, there is

$$\lambda = \frac{L}{L_0} \tag{2}$$

where L is is the gripper length after deformation, and L_0 is the original. We assume that the two-parameter Mooney-Rivlin model can transform the elastic strain energy W by

$$W = C_{10}(I_1 + 3) + C_{01}(I_2 - 3) \tag{3}$$

Among them, C_{10} and C_{01} are material parameters. I_1 and I_2 represent the isovolume invariants. Under the uniaxial conditions, I_1 and I_2can be represented by the following formula.

$$\begin{aligned} I_1 &= \lambda^2 + 2\lambda^{-1} \\ I_2 &= 2\lambda + \lambda^{-2} \end{aligned} \tag{4}$$

The second Piola-Kirchhoff stress in the tensile direction is represented as

$$T = 2\left(\frac{1}{\lambda} - \frac{1}{\lambda^4}\right)\left(\lambda\frac{\partial W}{\partial I_1} + \frac{\partial W}{\partial I_2}\right) \tag{5}$$

The first Piola-Kirchhofftress P and Cauchy stress Σ can be expressed as a function of the second Piola - Kirchhoff stress T by

$$\begin{aligned} P &= FT \\ \sigma &= J^{-1}FTF^{\intercal} \end{aligned} \tag{6}$$

where J is the volume ratio, and F is the deformation gradient matrix. Due to the incompressibility of the material ($J = 1$), F is an isotropic materials, which is given by the following formula.

$$F = \begin{bmatrix} \lambda & 0 & 0 \\ 0 & \frac{1}{\sqrt{\lambda}} & 0 \\ 0 & 0 & \frac{1}{\sqrt{\lambda}} \end{bmatrix} \tag{7}$$

According to equation (3-6), the first Piola-Kirchhoff stress P in the principal tensile direction can be expressed as

$$P = 2(1 - \lambda^{-3})(\lambda C_{10} + C_{01}) \tag{8}$$

C. Stress analysis

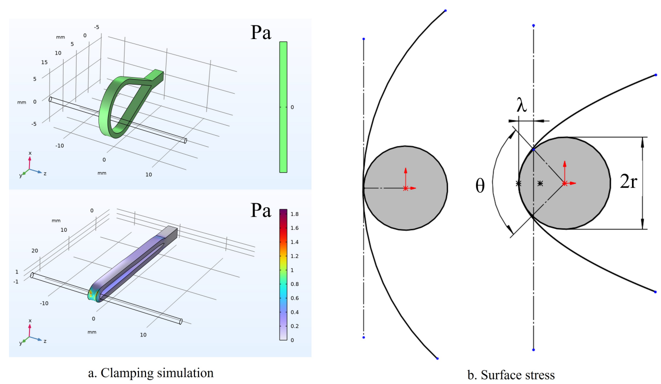

Fig. 3. The surface stress analysis

In order to simplify the calculation of the relationship between clamping force and strain, we use COMSOL simulation software to build a single finger model. The fixed finger is constrained as rigid object, and the pull finger is constrained as a hyperelastic object. The cylindrical guidewire passes through the middle part of the finger. The surface of the guidewire is tangent to the inner side of the finger, and the tangent point is at the centerline. Because of the interaction of other traction fingers, the position of guidewire is always fixed. So when dragging the fixed finger to clamp the guidewire, the pulling finger will deform and produce stress, as shown in Fig. 3(a).

Note that the friction force M acting on the guidewire in the radial direction is related to the clamping force N and friction coefficient μ, and its mathematical expression is

$$M = \mu N \tag{9}$$

While considering an infinitesimal arc area where the finger contacts the cylindrical surface, as shown in Fig. 3(b).

$$\mathrm{d}N = \frac{\pi r S P_c}{180}\mathrm{d}\theta \tag{10}$$

Where P_c represents the surface stress of the material and θ represents the angle of the furthest two points connecting lines from the centroid. λ represents the displacement of the finger. We can use the sector formula to calculate the relationship between θ and λ.

$$\cos(\frac{\theta}{2}) = \frac{r-\lambda}{r} \tag{11}$$

Assuming that the finger moves from θ_1 to θ_2, the maximum friction force f_v of a single finger on the guidewire can be calculated by the integral formula.

$$M(\theta_1,\theta_2) = \frac{\pi r \mu S P_c}{180}\int_{\theta_1}^{\theta_2}\theta d\theta \tag{12}$$

Bring equation (11) into equation (12) to get

$$\begin{aligned} M(\lambda_1,\lambda_2) = \frac{\pi S P_c \mu}{90}(\lambda_1 \arccos\lambda_1 - \sqrt{1-\lambda_1^2} \\ -\lambda_2 \arccos\lambda_2 + \sqrt{1-\lambda_2^2}) \end{aligned} \tag{13}$$

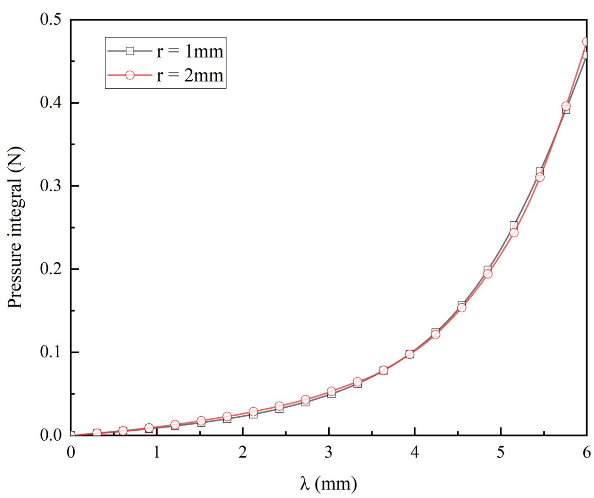

Fig. 4. The stress analysis of guidewires with different sizes

It is concluded that there is no correlation between the radius R of the clamped guidewire and the surface pressure M. We also prove this conclusion through the simulation results, as shown in Fig. 4.

III. Result Analysis

In order to verify the stress of different sizes paws, six kinds of fingers were selected by the method of controlled variables. The dimensions are shown in TABLE I.

In TABLE I, a, b, c, d, e and f represent the labels of fingers, respectively. Among them, a, b and c change the R value, which indicates that there are difference in the length of the finger; c, d and e change S value indicates that the width and number of finger are different; e and f by changing the value of D to change the thickness of the finger.

TABLE I
The pull finger sizes

Grippers (mm)	R	D	S
a	6	1	2
b	7	1	2
c	8	1	2
d	8	1	3
e	8	1	4
f	8	2	4

A. Grasping experiments

In the simulation process, a fixed constraints to the end of the gripper is added. And the surface of the guidewire is set to be rigid and contacted with the flexible gripper. The motion simulation process is shown in Fig. 5(a). For superelastic material parameters, a natural rubber with Shore hardness 40 is selected and shown in TABLE II.

TABLE II
Superelastic material parameters

Shore hardness	C_{10}(MPa)	C_{01}(MPa)
40	0.195	0.0162

In practical tasks, these parameters need to be obtained by experimental data. The purpose of this experiment is to determine the influence of different gripper shapes on stress and strain, so these parameters are set as fixed values. Then, a $6mm$ relative displacement is given between the catheter and the gripper, and the stress and strain is observed, as shown in Fig. 5(b).

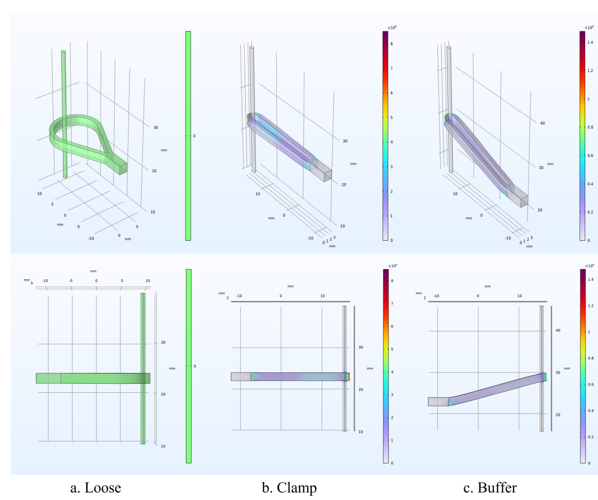

Fig. 5. The gripper motion simulation

In Fig. 6, the stress on the ordinate represents the clamping stress integral of the cylindrical surface of the guidewire. In order to ensure the consistency of units, all coordinates are divided by S, because for a single finger, the width of the

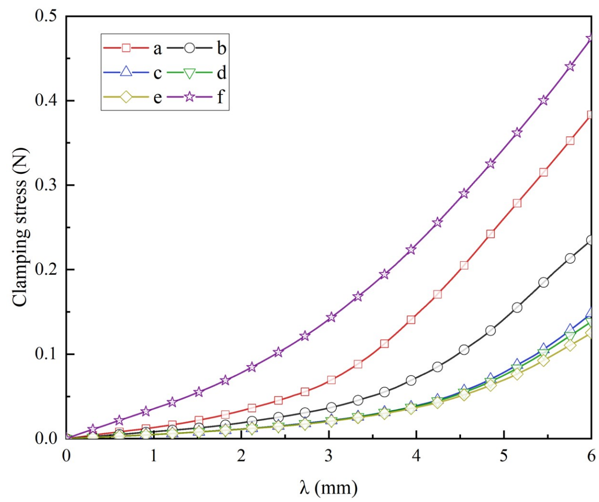

Fig. 6. The stress and strain in clamping state

whole gripper remains the same. The abscissa indicates the relative movement and displacement of the gripper and the catheter. Comparing curves e and f, increasing the thickness D of fingers can effectively improve the clamping force; Increasing the length R will make the fingers to relax; Increasing the width S will have a slight effect on the clamping force. Therefore, in order to ensure that the gripper does not slide relative to the guidewire, the most effective way to increase the gripper clamping force is to increase thickness and reduce the length. However, the excessive force may cause the damage. The solid gripper lacks stress buffering ability, so we have carried out the stress buffering experiment.

B. Buffering experiments

During the operation, the guidewire will contact with the blood vessel wall, resulting in stress. Experienced surgeons will make use of this power to achieve more dexterous and safe operations. For robot-assisted surgery, it takes a lot of cost to realize precise servo control, which is not conducive to be replaced. The flexible actuator proposed in this paper can play a role in buffering stress and strain, so as to reduce vascular injury.

From the grasping experiment, it can be seen that in a limited space, the force of the gripper is influenced by the structure of the finger. But the sensitivity to stress and strain is different. Under the action of radial displacement and friction force of guidewires, the clamping finger is tightened in the radial direction, as shown in Fig. 5(c). According to the interaction of forces, the strain of the gripper is consistent with the sudden stress of the guidewire when moving in the blood vessel. During the process of operation, if the gripper is deformed more due to the same force, we consider that the sensitivity is higher. Then, a $6mm$ movement is given on radial direction of the guidewire, and the stress-strain relationship of the finger is observed, as shown Fig. in 7.

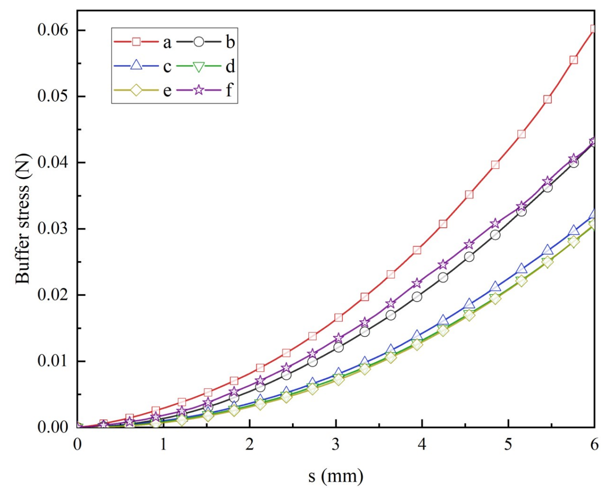

Fig. 7. The stress and strain in buffered state

In Fig. 7, in order to ensure that the change of longitudinal coordinate of the guidewire is more consistent, the change of longitudinal coordinate is divided by the radial coordinate, so that all the longitudinal coordinates can represent the initial stress of the catheter. The abscissa represents the radial displacement of fingers. Comparing curves c,d and e, it can also be seen that increasing width S has only slight influence on the stress; According to a, b and c, increasing the length R will improve the sensitivity of grippers; Compared with e and f, increasing the thickness D will reduce the sensitivity of the gripper, but not as obvious as R.

IV. Discussion

The above two experimental results show that, in a limited space, if the size of the gripper is reasonably selected, the effective buffer can be provided for the stress of the guidewire while maintaining sufficient clamping force. Some researchers show that the finger holding force over $3N$ can be competent for the operation. According to the Fig. 6, pulling the finger with curve a $(0.383 \times 12 = 4.596N)$ and curve f $(0.473 \times 12 = 5.676N)$ in the relative movement space $(6 \times 2 = 12mm)$ can meet the requirements. Here, it is 12 because the clamping force are tangent and cancel each other out in the guidewire, and the position of the guidewire remains the same during the process. During the process of operation, assuming that the maximum sensitive force range of the gripper in $6mm$ space does not exceed $2N$, the stress distributed to a single finger should be $(2/24 \approx 0.08N)$. As can be seen from the Fig. 7, all pulling fingers can meet the requirements. Here, it is 24 because the clamping force acts on the radial direction of the guidewire, and the shear is superimposed on each other. If it is required that the maximum sensitive stress range should not exceed $1N$, and the stress allocated to a single finger shall be $(1/24 \approx 0.04N)$, then the traction finger a $(0.0602N)$, traction finger b $(0.0430N)$ and traction finger f $(0.0432N)$ can not meet the requirements. At this time, if the pulling finger c is selected, once the radial force of the guidewire exceeds $0.032 \times 24 = 0.768N$, the guidewire will slide relative to the pulling finger to ensure that the blood vessel will not be punctured. However, there are still some problems. The superelastic materials in this paper are all assumed, and the parameters need to be further confirmed in the real environment.

V. Conclusion

In this paper, a parallel multi-fingered flexible gripper structure based on vascular intervention robot was proposed. Compared with mechanical gripper, the flexible gripper achieved enough force in a narrow space without damaging the guidewire/catheter. Furthermore, the flexible gripper can provide a buffer zone in the guidewire/catheter moving direction, It will reduce the effect of sudden stress and avoid vascular injury in real time. The simulation results by Mooney-Rivlin model show that the proposed method is suitable for different sizes of surgical instruments. The volume of the buffer zone varies with the length, width and thickness of grippers. These results provide a reference for the setting of the srugery robot's grasping range. In the future, a reasonable model with materials will be constructed to meet the real environments of vascular intervention surgery.

Acknowledgment

This work was supported in part by the National Natural Science Foundation of China (61703305), in part by National High-tech Research and Development Program (863 Program) of China (2015AA043202), in part by SPS KAKENHI (15K2120) in part by Key Research Program of the Natural Science Foundation of Tianjin (18JCZDJC38500), and in part by Innovative Cooperation Project of Tianjin Scientific and Technological Support (18PTZWHZ00090).

References

[1] P. Shi, S. Guo, L. Zhang, X. Jin, H. Hirata, T. Tamiya, and M. Kawanishi, "Design and Evaluation of a Haptic Robot-Assisted Catheter Operating System With Collision Protection Function," *IEEE Sensors J.*, vol. 21, no. 18, pp. 20 807–20 816, Sep. 2021.

[2] X. Jin, S. Guo, J. Guo, P. Shi, T. Tamiya, M. Kawanishi, and H. Hirata, "Total Force Analysis and Safety Enhancing for Operating Both Guidewire and Catheter in Endovascular Surgery," *IEEE Sensors J.*, vol. 21, no. 20, pp. 22 499–22 509, Oct. 2021.

[3] X. Li, S. Guo, P. Shi, X. Jin, and M. Kawanishi, "An Endovascular Catheterization Robotic System Using Collaborative Operation with Magnetically Controlled Haptic Force Feedback," *Micromachines*, vol. 13, no. 4, p. 505, Apr. 2022.

[4] S. Guo, Y. Song, X. Yin, L. Zhang, T. Tamiya, H. Hirata, and H. Ishihara, "A Novel Robot-Assisted Endovascular Catheterization System With Haptic Force Feedback," *IEEE Transactions on Robotics*, vol. 35, no. 3, pp. 685–696, Jun. 2019.

[5] C. Yang, S. Guo, and X. Bao, "An isomorphic interactive device for the interventional surgical robot after in vivo study," *Micromachines*, vol. 13, no. 1, 2022.

[6] C. Yang, S. Guo, Y. Guo, and X. Bao, "Cloud communication-based sensing performance evaluation of a vascular interventional robot system," *IEEE Sensors Journal*, pp. 1–1, 2022.

[7] W. Zhou, S. Guo, J. Guo, F. Meng, and Z. Chen, "ADRC-Based control method for the vascular intervention Master–Slave surgical robotic system," *Micromachines*, vol. 12, no. 12, 2021.

[8] W. Zhou, S. Guo, J. Guo, F. Meng, Z. Chen, and C. Lyu, "A Surgeon's Habits-Based Novel Master Manipulator for the Vascular Interventional Surgical Master-Slave Robotic System," *IEEE Sensors Journal*, vol. 22, no. 10, pp. 9922–9931, 2022.

[9] J. Guo, X. Jin, S. Guo, and Q. Fu, "A Vascular Interventional Surgical Robotic System Based on Force-Visual Feedback," *IEEE Sensors Journal*, vol. 19, no. 23, pp. 11 081–11 089, 2019.

[10] X. Jin, S. Guo, J. Guo, P. Shi, T. Tamiya, and H. Hirata, "Development of a tactile sensing robot-assisted system for vascular interventional surgery," *IEEE Sensors Journal*, vol. 21, no. 10, pp. 12 284–12 294, 2021.

[11] X. Jin, S. Guo, J. Guo, P. Shi, M. Kawanishi, and H. Hirata, "Active Suppression Method of Dangerous Behaviors for Robot-Assisted Vascular Interventional Surgery," *IEEE Transactions on Instrumentation and Measurement*, vol. 71, pp. 1–9, 2022.

[12] S. Guo, Y. Wang, Y. Zhao, J. Cui, Y. Ma, G. Mao, and S. Hong, "A Surgeon's Operating Skills-Based Non-Interference Operation Detection Method for Novel Vascular Interventional Surgery Robot Systems," *IEEE Sensors Journal*, vol. 20, no. 7, pp. 3879–3891, Apr. 2020.

[13] X. Bao, S. Guo, Y. Guo, C. Yang, L. Shi, Y. Li, and Y. Jiang, "Multilevel Operation Strategy of a Vascular Interventional Robot System for Surgical Safety in Teleoperation," *IEEE Transactions on Robotics*, pp. 1–13, 2022.

[14] Y. Yan, H. Wang, H. Yu, F. Wang, J. Fang, J. Niu, and S. Guo, "Machine learning-based surgical state perception and collaborative control for a vascular interventional robot," *IEEE Sensors Journal*, vol. 22, no. 7, pp. 7106–7118, 2022.

[15] S. Guo, J. Cui, Y. Zhao, Y. Wang, Y. Ma, W. Gao, G. Mao, and S. Hong, "Machine learning-based operation skills assessment with vascular difficulty index for vascular intervention surgery," *Med Biol Eng Comput*, vol. 58, no. 8, pp. 1707–1721, Aug. 2020.

[16] Y. Zhao, H. Xing, S. Guo, Y. Wang, J. Cui, Y. Ma, Y. Liu, X. Liu, J. Feng, and Y. Li, "A novel noncontact detection method of surgeon's operation for a master-slave endovascular surgery robot," *Med Biol Eng Comput*, vol. 58, no. 4, pp. 871–885, Apr. 2020.

[17] Y. Zhao, S. Guo, Y. Wang, J. Cui, Y. Ma, Y. Zeng, X. Liu, Y. Jiang, Y. Li, L. Shi, and N. Xiao, "A CNN-based prototype method of unstructured surgical state perception and navigation for an endovascular surgery robot," *Med Biol Eng Comput*, vol. 57, no. 9, pp. 1875–1887, Sep. 2019.

[18] N. Rojas, R. R. Ma, and A. M. Dollar, "The GR2 gripper: An underactuated hand for open-loop in-hand planar manipulation," *IEEE Transactions on Robotics*, vol. 32, no. 3, pp. 763–770, 2016.

[19] K. Morino, S. Kikuchi, S. Chikagawa, M. Izumi, and T. Watanabe, "Sheet-based gripper featuring passive pull-in functionality for bin picking and for picking up thin flexible objects," *IEEE Robotics and Automation Letters*, vol. 5, no. 2, pp. 2007–2014, 2020.

[20] J. M. Krahn, F. Fabbro, and C. Menon, "A soft-touch gripper for grasping delicate objects," *IEEE/ASME Transactions on Mechatronics*, vol. 22, no. 3, pp. 1276–1286, 2017.

[21] X. Zheng, N. Hou, P. J. Daniël Dinjens, R. Wang, C. Dong, and G. Xie, "A thermoplastic elastomer belt based robotic gripper," in *2020 IEEE/RSJ International Conference on Intelligent Robots and Systems (IROS)*, 2020, pp. 9275–9280.

[22] W. Yuan, S. Dong, and E. H. Adelson, "GelSight: High-resolution robot tactile sensors for estimating geometry and force," *Sensors*, vol. 17, no. 12, 2017.

[23] Q. Liu, X. Gu, N. Tan, and H. Ren, "Soft robotic gripper driven by flexible shafts for simultaneous grasping and in-hand cap manipulation," *IEEE Transactions on Automation Science and Engineering*, vol. 18, no. 3, pp. 1134–1143, 2021.